Available online at www.sciencedirect.com
ScienceDirect
Journal of Molecular Graphics and Modelling 26 (2007) 720–727
Journal of Molecular Graphics and Modelling
www.elsevier.com/locate/JMGM

Insight into analysis of interactions of saquinavir with HIV-1 protease in comparison between the wild-type and G48V and G48V/L90M mutants based on QM and QM/MM calculations

Suwipa Saen-oon [a,1], Ornjira Aruksakunwong [b], Kittiyaporn Wittayanarakul [a], Pornthep Sompornpisut [a], Supot Hannongbua [a,*]

[a] Department of Chemistry, Faculty of Science, Chulalongkorn University, Prathumwan, Bangkok 10330, Thailand
[b] Department of Chemistry, Faculty of Science, Rangsit University, Muang-Ake, Phaholyothin Road, Lak-Hok, Pathumtani 12000, Thailand

Received 12 December 2006; received in revised form 19 April 2007; accepted 28 April 2007
Available online 3 May 2007

Abstract

Saquinavir (SQV) was the first HIV-1 PR inhibitor licensed for clinical use and widely used for acquired immunodeficiency syndrome (AIDS) therapy. Its effectiveness, however, has been hindered by the emergence of resistant mutations. The two most important HIV-1 PR mutants are G48V and G48V/L90M. Inhibition studies of SQV on these mutants demonstrated 13.5- and 419-fold reductions of susceptibility, respectively. In this study, an analysis of energetic binding affinity between saquinavir and the HIV-1 PR wild-type and these two mutants has been performed in detail based on density functional theory and the hybrid quantum mechanical/molecular mechanical (QM/MM) calculations. We have found that the interaction of SQV with flap residue 48 of the mutants is significantly perturbed, as shown by the reduced stability of binding between SQV and residue 48 for the G48V and G48V/L90M mutants over the wild-type. This was associated with conformational changes of the inhibitor and the enzyme, leading to the loss of hydrogen bonding between the binding subsite P2 and the backbone carbonyl of residue 48. Moreover, the G48V/L90M mutations cause the repositioning of the residues close to residues 48 and 90, at important locations as a part of the flap and catalytic regions, respectively. The repositioning of these residues consequently perturbed the binding affinity of SQV in the pocket as indicated by the decreasing interaction energies. In addition to the loss of inhibitor/enzyme binding, it is interesting to observe that the mutation leads significantly to an increase of the stability of the enzyme.

Keywords: HIV-1 protease; Saquinavir; Molecular dynamics simulations; Mutation; ONIOM method

1. Introduction

The acquired immunodeficiency syndrome (AIDS) has become a serious global concern due to an increasing number of HIV patients and infected population all over the world. Since it was first recognized in 1981, the disease has never been completely cured. AIDS is caused by the human immunodeficiency virus (HIV). The replication cycle of the virus involves three essential enzymes, reverse transcriptase (RT), protease (PR) and integrase (IN). The three enzymes are become important targets for drug development. Effective drugs were developed against HIV-1 PR and HIV-1 RT; however, it was found that inhibitors at the first target are more potent [1]. Therefore, HIV-1 PR is an attractive target for antiviral therapy.

The HIV type I protease (HIV-1 PR) is a member of the aspartic protease family. The enzyme is a homodimer consisting of 99 amino acids. The active site contains two conserved active site residues, D25 and D25′. Interfacial contact between the subunits allows two crucial substrate binding clefts to be formed. They include the catalytic triad residues D25–T26–G27 on one side and the flap loop residues 46–54 on the other (Fig. 1). To date, ten HIV-1 PR inhibitors have been approved by the United Stated Food and Drug Administration (FDA), and are in clinical use. Saquinavir (SQV) is considered to be highly potent and selective to HIV-1 PR inhibitor [2]. It is classified as a peptidomimetic protease

* Corresponding author. Tel.: +66 2 2187603; fax: +66 2 2187603.
E-mail address: supot.h@chula.ac.th (S. Hannongbua).
[1] Present address: Department of Physiology and Biophysics, Albert Einstein College of Medicine, 1300 Morris Park Avenue, Bronx, NY 10461, United States.

1093-3263/$ – see front matter © 2007 Elsevier Inc. All rights reserved.
doi:10.1016/j.jmgm.2007.04.009

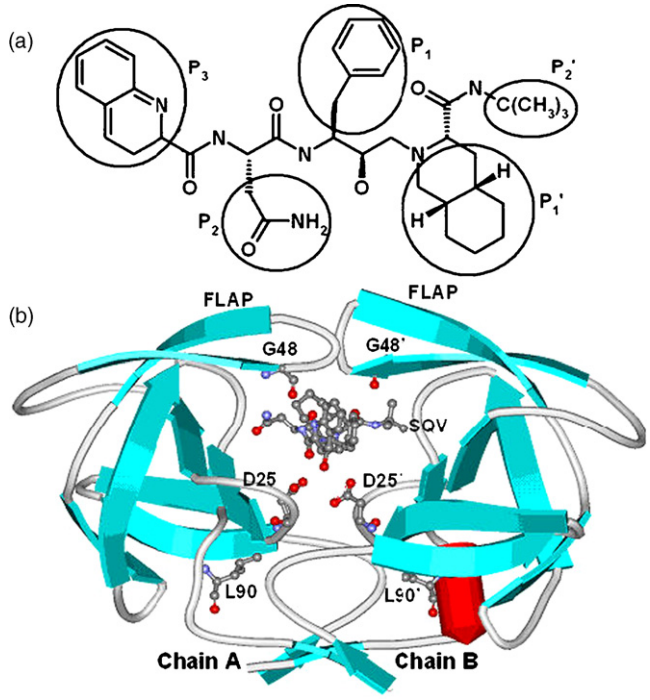

Fig. 1. Schematic representations of (a) saquinavir (SQV) and (b) the wild-type HIV-1 PR/SQV complex. According to the conventional classification, the protease subsites are designated by the inhibitor side chains P_1, P_2, P_3, P'_1 and P'_2. The catalytic dyad, D25 and D25′, as well as the major mutation residues, G48, G48′, L90 and L90′, are displayed as balls and sticks.

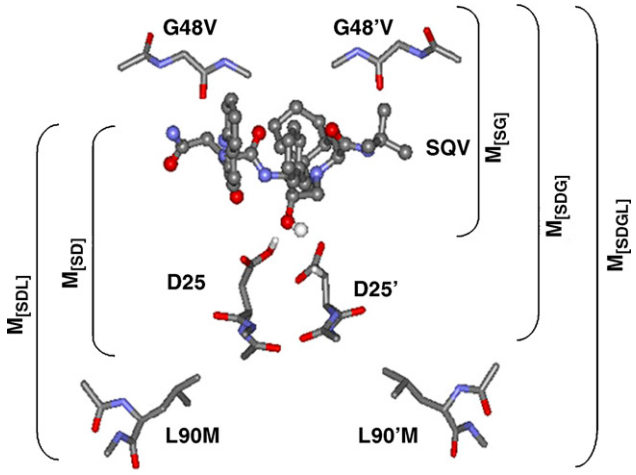

Fig. 2. Schematic structure representation of the quantum model for the interaction energy calculations, where saquinavir (SQV), the catalytic dyad (D25 and D25′) as well as the major mutations, G48V, G48′V, L90M and L90′M, are displayed (see text for more details).

inhibitor. The inhibitor contains a nonhydrolyzable hydroxyethylene isostere which was designed based on the transition state structure in the enzyme-substrate complex (Fig. 2).

There has been strong evidence that inappropriate treatment of HIV medications could result in sequential acquisition of drug resistant mutation. Genotypic and phenotypic resistance mutations of HIV-1 PR from the Stanford HIV database include almost 50% of the residues, and over 20 residues are associated with resistance to clinically available inhibitors [3], Recently, a correlation between inhibitor structure of the HIV-1 PR target and drug resistance was studied. Kinetic experiments show that the decreased affinity of drugs for many mutants is caused by an increase in dissociation rates [4]. The HIV-1 PR mutant species of the single mutation, G48V, and double mutation, G48V/L90M, are associated *in vivo* with saquinavir resistance by the enzyme [5] and kinetic studies on these mutants demonstrate 13.5- and 419-fold increases in K_i values, respectively, compared with the wild-type enzyme. Residue G48 is located in the flaps of the protease and contributes to the formation of the S_2/S'_2 and S_3/S'_3 binding sites the regions of the enzyme that bind with P_2/P'_2 and P_3/P'_3 of the inhibitor, respectively [6], but residue 90 does not directly make contact with the inhibitor.

Our previous molecular dynamics and quantum chemical calculations [7] showed that conformational change of the subsite P_2 of the G48V-SQV complex results in a decrease of interaction energy between this subsite and residue 48 [2]. This observation was supported by X-ray data where the authors stated that more space was needed in the P_3 subsite in order to accommodate the side chain of valine for the G48V mutation [2]. In this report, we employed extensive computations using density functional theory (DFT) and a hybrid quantum mechanical/molecular mechanical (QM/MM) method namely the Our own N-layered Integrated molecular Orbital and Molecular mechanics method (ONIOM) approach to calculate the interaction energy of an entire set and individual pairs of the systems. The studied systems included the HIV-1 PR wild-type and G48V and G48V/L90M mutants complexed with SQV. These mutations are more frequently found in patients treated with SQV. Viruses containing both G48V and L90M mutations result in an enzyme highly resistant to SQV. The inhibition constant (K_i) of the double mutant is 419 times less sensitive to SQV as compared with that of the wild-type [8].

2. Computational methods

A combination of different computational methodologies was applied in order to provide detailed insight into the structural, dynamical and energetic properties among the three complexes of HIV-1 PR/SQV which are (i) the wild-type (WT), (ii) a single mutation at residue 48 from glycine to valine (G48V) and (iii) the double mutation at residues 48 and 90 from glycine to valine and leucine to methionine, respectively (G48V/L90M). The molecular dynamics simulations were carried out and then followed by the quantum chemical calculations for extensively interaction energy analysis.

2.1. Molecular dynamics simulations

The WT, G48V single- and G48V/L90M double-mutant HIV-1 PR complexed with saquinavir inhibitor were constructed from the X-ray structure (Protein Data Bank code 1HXB; 2.3 Å resolutions). The protein was assigned to a monoprotonation state, in which the proton attaches to the carboxyl sidechain of D25. The TIP3P water molecules [9] were used to solvate the complexes. Sodium and chloride ions were added to neutralize the system. The force field parameters

of molecular mechanics bonded-type and van der Waals potentials for saquinavir were assigned using AntechAmber [10]. Their partial atomic charges were obtained from a restrained SQV structure that was partially optimized at the Hartree-Fock level with 6-31G* basis functions to adjust the bond lengths involving hydrogen atoms. Then, the RESP fitting procedure was employed to calculate partial atomic charges of the inhibitor [11,12]. Gaussian 98 [13] was used to optimize the molecular structure, generate electrostatic potentials, and calculate ab initio energies. This method is the same as that used to prepare the parameters of amino acids in the AMBER 7.0 program.

Energy minimizations were carried out to relax the model prior to MD runs. A cutoff distance of 12 Å was applied for non-bonded pair interactions. The Particle Mesh Ewald (PME) method was employed to correct for electrostatic interactions. The simulation time step was set at 2 fs. The temperature of the model was gradually raised to 298 K for the first 60 ps, then, kept constant until 1 ns.

The molecular mechanics potential energy minimizations and MD simulations were carried out using the AMBER 7.0 simulation package [14]. Calculations were performed using the parm99 force field. All MD runs reported here were performed under an isobaric-isothermal ensemble (NPT) using a constant pressure of 1 atm and constant temperature of 298 K [15].

2.2. Quantum mechanical calculations

In this study, we focused mainly on a high-level energy evaluation of the model systems involving SQV, the catalytic D25/D25′ and the primary residue mutations. An average structure obtained from the MD trajectory was used as a representative structure for the simulated system. The partial optimization using the B3LYP/6-31G(d,p) were performed by constrain the heteroatom to keep the configuration as obtained from MD simulations. The representative structure of each set was used to construct five model systems, which we denote as $M_{[SD]}$, $M_{[SG]}$, $M_{[SDG]}$, $M_{[SDL]}$ and $M_{[SDGL]}$, where the subscripts S, D, G and L refer to SQV, D25 and D25′, G48 and G48′, and L90 and L90′, respectively (Fig. 2). For the G48V and G48V/L90M mutants, the G and L confer to V (valine) and M (methionine), respectively. Therefore, a total of 15 model systems were generated for the energy evaluation.

Potential energies of all model systems were computed for constrain configurations using quantum chemical (QM) calculations at the B3LYP/6-31G(d,p) level with the additional diffusion function assigned to only four oxygen atoms of D25 and D25′. Here, the Gaussian 98 program was used [13].

The interaction energy of the complex of the model system (ΔE_{cpx}) is defined by subtraction of the total energy of the n isolated monomers existing in the complex (E_i) from that of the complex (E_{cpx}) using the following equation:

$$\Delta E_{cpx} = E_{cpx} - \sum_{i=1}^{n} E_i \quad (1)$$

For instance, ΔE_{cpx} for $M_{[SGDL]}$ of the WT model represents the overall interaction between SQV and D25, D25′, G48, G48′, L90 and L90′. The corresponding set of residues is SQV, D25, D25′, V48, V48′, L90 and L90′ for G48V or SQV, D25, D25′, V48, V48′, M90 and M90′ for G48V/L90M.

The model $M_{[SD]}$ is to truncate only the interaction between SQV and the catalytic residues, D25 and D25′. To include the effect of the primary mutated residues at the flap region, G48(V) and G48′(V), in to the $M_{[SD]}$, the $M_{[SDG]}$ model was proposed. This enables us to measure the interaction characteristics of SQV in the presence of both the catalytic dyad and mutated residue at the flap region. In the same manner, $M_{[SDL]}$ was set up to focus on the effect of the mutated residues L90M and L90′M. In addition to $M_{[SDL]}$, the SQV and catalytic dyad as well as the double mutated residues that cause extreme resistance (~419-fold over wild-type) were included in the $M_{[SDGL]}$ model.

2.3. ONIOM calculations

The Our-own N-layered Integrated molecular Orbital and Molecular mechanics (ONIOM) method, which developed by Morokuma [16], has been introduced and its efficiency has been improved. Simply put the concept of the ONIOM approach is to partition the large molecular system into onion-skin-like layers, using different combinations of the quantum chemical methods and molecular mechanics methods for different layers of the system partitioning [17,18].

In the present study, three-layered ONIOM calculations (denoted as ONIOM3) were used. A schematic representation of the ONIOM concept is presented in Fig. 3.

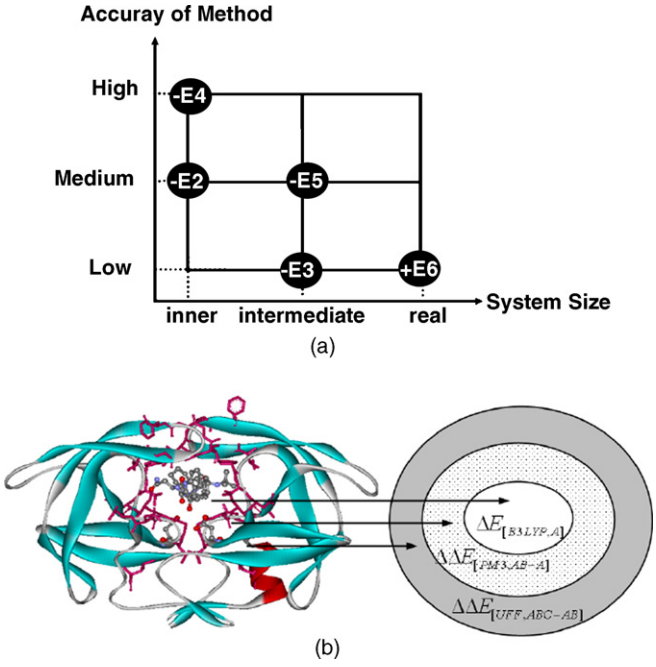

Fig. 3. Schematic representation of the three-layer ONIOM (a) extrapolation scheme and (b) calculated levels (see text for more details).

The total energy from the three-layer ONIOM can be obtained from five independent calculations:

$$E^{\mathrm{ONIOM3}} = E[Low, real] + E[Med, \mathrm{int}] + E[High, inner] - E[Low, \mathrm{int}] - E[Med, inner] = E6 + E5 + E4 - E3 - E2, \quad (2)$$

where *real* denotes the entire system, which is treated at the *low* level, while *int* denotes the part of the system partitioned to be the *intermediate* layers for which the energy is calculated at both the *medium* and *low* levels. Here inner denotes the *inner* layer of the system partitioning, whose energy is calculated at both *high* and *medium* levels.

The HIV-1 PR/SQV complex was divided into three parts represented by the *inner* layer (A), *intermediate* layer (AB) and *real* layer (ABC) (Fig. 3b). The *inner* layer (A), with ball and stick model shown in Fig. 3, representing the direct binding of SQV to the catalytic dyad (D25/D25′), flap region (G48/G48′) and L90/L90′. They were treated at the high level of QM calculation using density functional theory (B3LYP/6-31G(d,p)). The *intermediate* layer (AB) covers all amino acids of both chains of the HIV-1 PR lying within 5 Å from any atom of SQV. This layer, containing 36 amino acids, was treated with the lower level of calculation, a semiempirical method (PM3) (Fig. 3). The real layer (ABC) takes into account the entire enzyme system. It was carried out by the molecular mechanics (MM) method using a universal force field (UFF). Configurations taken from the averaged MD structures of the HIV-1 PR/SQV complex were used. All ONIOM calculations were carried out using the Gaussian 98 program package.

Here, the interaction energy (ΔE) between SQV and the HIV-1 PR was defined by:

$$\Delta E = E_{\mathrm{complex}} - E_{\mathrm{PR}} - E_{\mathrm{SQV}}, \quad (3)$$

where E_{complex}, E_{PR} and E_{SQV} represent the total energy of the HIV-1 PR/SQV complex, HIV-1 PR and SQV, respectively. Hence, the total energy obtained from the ONIOM3 calculations (E^{ONIOM3}) herein can be expressed as:

$$E^{\mathrm{ONIOM3}}[\mathrm{ABC}] = E_{[\mathrm{UFF,ABC}]} + E_{[\mathrm{PM3,AB}]} + E_{\mathrm{B3LYP,A}} - E_{[\mathrm{UFF,AB}]} - E_{[\mathrm{PM3,A}]}, \quad (4)$$

Therefore, the total interaction energy ($\Delta E^{\mathrm{ONIOM3}}_{\mathrm{total}}[\mathrm{ABC}]$) can be written by the expression of independent energy components as follows:

$$\Delta E^{\mathrm{ONIOM3}}_{\mathrm{total}}[\mathrm{ABC}] = \Delta E_{[\mathrm{UFF,ABC}]} + \Delta E_{[\mathrm{PM3,AB}]} + \Delta E_{[\mathrm{B3LYP,A}]} - \Delta E_{[\mathrm{UFF,AB}]} - \Delta E_{[\mathrm{PM3,A}]} \quad (5)$$

$$\Delta E^{\mathrm{ONIOM3}}_{\mathrm{total}}[\mathrm{ABC}] = \Delta E_{[\mathrm{B3LYP,A}]} + \Delta\Delta E_{[\mathrm{PM3,AB\text{-}A}]} + \Delta\Delta E_{[\mathrm{UFF,ABC\text{-}AB}]}, \quad (6)$$

where $\Delta E_{[\mathrm{B3LTP,A}]}$ is the interaction energy in the region A, particularly for the direct interaction between SQV and the catalytic dyad residues, D25 and D25′, evaluated at the B3LYP/6-31G(d,p) level. $\Delta\Delta E_{[\mathrm{PM3,AB\text{-}A}]}$ is the interaction energy between the regions A and B evaluated at the PM3 level, and $\Delta\Delta E_{[\mathrm{UFF,ABC\text{-}AB}]}$ represents the interaction between regions AB and C evaluated by molecular mechanics (UFF), all for the HIV-1 PR/SQV complex.

3. Results and discussion

3.1. Stability of the WT, G48V and G48V/L90M complexes: QM calculations

The calculated total interaction energy of SQV with the residues according to each studied model is shown in Table 1 by comparison between the wild-type and the two mutants. The relative interaction energy ($\Delta\Delta E$) of the G48V single and G48V/L90M double mutant with respect to the interaction energy of the wild-type system is given in parentheses. For $M_{[\mathrm{SGDL}]}$ representing the interaction of the complex where the *inner* layer contains SQV and 6 residues, the results indicate a large destabilization energy of 17.8 kcal/mol over the wild-type caused by the G48V/L90M double mutant. On the other hand, the G48V single mutant gives only a minor decrease in binding energy for the overall complex system (0.9 kcal/mol). The results of this comparison in terms of the interaction energy are quite consistent with the small degree of resistance (13.5-fold) for the G48V single mutant and strong resistance (419-fold) for the G48V/L90M double mutants, compared with the wild-type enzyme.

Consider the interaction energy components due to mutations obtained from the $M_{[\mathrm{SD}]}$ and $M_{[\mathrm{SG}]}$ models. The interactions at the flap region ($\Delta E_{(\mathrm{SQV+G48V+G48'V})}$) are in the order WT > G48V ≫ G48V/L90M with the corresponding

Table 1
The total interaction energy of saquinavir with amino acid residues D25, D25′, G48(v), G48′(V), L90(M) and L90′(M) for the WT, G48V and G48V/L90M mutants

Model		Interaction energy (kcal/mol)				
		WT	G48V	$(\Delta\Delta E)^{a}$	G48V/L90M	$(\Delta\Delta E)^{a}$
$M_{[\mathrm{SGDL}]}$	$\Delta E_{(\mathrm{cpx})}$	−57.5	−56.6	0.9	−39.7	17.8
$M_{[\mathrm{SD}]}$	$\Delta E_{(\mathrm{SQV+D25+D25'})}$	−34.2	−37.3	−3.1	−31.0	3.2
$M_{[\mathrm{SG}]}$	$\Delta E_{(\mathrm{SQV+G48V+G48'V})}$	−15.7	−12.2	3.5	−2.9	12.8
$M_{[\mathrm{SGD}]}$	$\Delta E_{(\mathrm{SQV+D25+D25'+G48V+G48'V})}$	−50.2	−49.2	1.0	−25.3	24.9
$M_{[\mathrm{SDL}]}$	$\Delta E_{(\mathrm{SQV+D25+D25'+L90M+L90'M})}$	−43.5	−44.8	−1.3	−41.8	1.7

[a] $(\Delta\Delta E) = \Delta E_{\mathrm{mutant}} - \Delta E_{\mathrm{WT}}$.

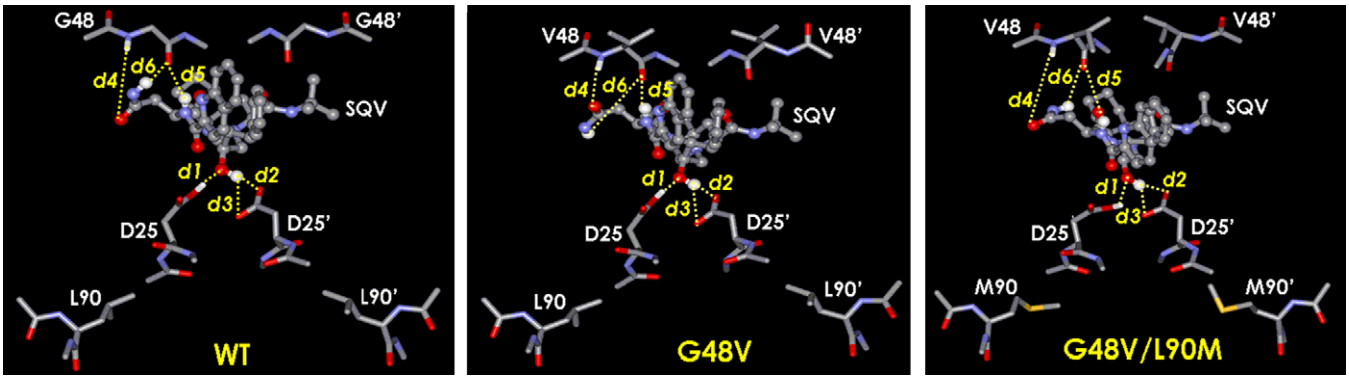

Fig. 4. Hydrogen bond distances (*di*, where $i = 1$–6) between saquinavir (SQV) and the catalytic dyad (D25 and D25′) as well as the major mutation residues (G48, G48′, L90 and L90′) for the three simulated systems, the wild-type (WT) and G48V and G48V/L90M mutants.

energies of −15.7, −12.2 and −2.9 kcal/mol, respectively. This is not the case for the catalytic region in which the order of $\Delta E_{(SQV+D25+D25')}$ is G48V > WT > G48V/L90M with the interaction energies of −37.3, −34.2 and −31.0 kcal/mol, respectively.

The above data suggest that the destabilization of the SQV binding in the mutant complexes has a larger contribution from the particular interaction of SQV with the flap residues than that with the catalytic residues (Table 1). The structure of SQV in the PR binding pocket is shown in Fig. 4 comparing the WT, G48V and G48V/L90M species and the important hydrogen bonds.

In order to gain insight into the detailed interaction between each pair-residue at the flap and catalytic regions (models $M_{[SDG]}$ and $M_{[SDL]}$), the decomposition of interaction energies into pair interactions was calculated and given separately in Tables 2 and 3. The interaction of SQV with the flap residue 48 is significantly perturbed due to the mutations. As can be seen from Table 2, the stabilities of G48V and G48V/L90M were reduced by 3.5 and 12.8 kcal/mol relative to that of WT (model $M_{[SG]}$). This observation can be understood by the loss of hydrogen bonding between the P_2-subsite of SQV and the backbone of residue 48 (details are provided in Section 3 for the hydrogen bonding observations from MD simulations). In addition to the loss of inhibitor/enzyme binding, it is interesting to observe that the mutation leads to a substantial increase of the stability of the enzyme. As can be seen from the $M_{[SDG]}$ model, the total interaction between the 4 residues ($\Delta E_{(25+25'+48+48')}$), D25, D25′, G48(V) and G48′(V), increases significantly from −7.4 to −21.2 kcal/mol when changing from WT to the G48V/L90M mutation.

As found for the flap domain in Table 2 (model $M_{[SDG]}$), a similar increase in the binding stability at the catalytic region due to the mutation can be also observed for the model $M_{[SDL]}$. As can be seen in Table 3, double mutations lead to a substantial increase of the total residue-residue interactions in the (25 + 25′ + 90 + 90′) and (25 + 25′) clusters. Interaction among the 4 residues (25 + 25′ + 90 + 90′) was increased from −16.2 to −16.6 and −33.4 kcal/mol in changing from WT to single and double mutations, respectively. The corresponding values for the catalytic (25 + 25′) cluster are −8.7, −8.8 and −21.9 kcal/mol.

Although the overall interaction energies ($\Delta E_{(SQV+25+25'+90+90')}$) for the saquinavir bound to the catalytic part of both G48V (−44.8 kcal/mol) and G48V/L90M (−41.8 kcal/mol) are not substantially different from that of −43.5 kcal/mol of the wild-type, the analysis of the distribution of the total interaction energy among the various components gives some insight into the contributions to the interaction energy of the system. From Table 3, it can be clearly seen that the mutated methionine side chain at position 90 leads to the destabilization of the D25/saquinavir interaction by 10.7 kcal/mol compared with the wild-type. This could be due to van der Waals interactions between its side chain and the main-chain

Table 2
The decomposition of pair interactions of the flap region: (SQV + 25 + 25′ + 48 + 48′) and (SQV + 48 + 48′) systems

Model	Interaction energy (kcal/mol)				
	WT	G48V		G48V/L90M	
$M_{[SDG]}$					
$\Delta E_{(SQV+25+25'+48+48')}$	−50.2	−49.2	1.0	−25.3	24.9
$\Delta E_{(25+25'+48+48')}$	−7.4	−8.4	−1.0	−21.2	−13.8
$M_{[SG]}$					
$\Delta E_{(SQV+48+48')}$	−15.7	−12.2	3.5	−2.9	12.8
$\Delta E_{(SQV+48)}$	−11.7	−8.2	3.5	−2.1	9.6
$\Delta E_{(SQV+48')}$	−4.1	−3.4	0.7	−0.9	3.2
$\Delta E_{(48+48')}$	0.0	0.1	0.1	0.09	0.1

Table 3
The decomposition of pair interactions of the catalytic region: (SQV + 25 + 25′ + 90 + 90′) and (SQV + 25 + 25′) systems

Model	Interaction energy (kcal/mol)				
	WT	G48V		G48V/L90M	
$M_{[SDL]}$					
$\Delta E_{(SQV+25+25'+90+90')}$	−43.5	−44.8	−1.3	−41.8	1.7
$\Delta E_{(25+25'+90+90')}$	−16.2	−16.6	−0.4	−33.4	−17.2
$M_{[SD]}$					
$\Delta E_{(SQV+25+25')}$	−34.2	−37.3	−3.1	−31.0	3.2
$\Delta E_{(SQV+25)}$	−8.0	−8.0	−0.0	2.7	10.7
$\Delta E_{(SQV+25')}$	−16.1	−19.2	−3.1	−16.3	−0.2
$\Delta E_{(25+25')}$	−8.7	−8.8	−0.1	−21.9	−13.2

Table 4
The many-body interaction energy (kcal/mol) for the model $M_{[SDG]}$ of the wild-type

WT	Interaction energy
$\Delta E_{(SQV+D25+25'+48+48')}$	−50.2
ΔE_{pairs}	
$\Delta E_{(SQV+25)}$	−8.0
$\Delta E_{(SQV+25')}$	−16.1
$\Delta E_{(25+25')}$	−8.7
$\Delta E_{(SQV+48)}$	−11.7
$\Delta E_{(SQV+48')}$	−4.1
$\Delta E_{(48+48')}$	0.0
$\Delta E_{(25+48)}$	0.0
$\Delta E_{(25+48')}$	−0.1
$\Delta E_{(25'+48)}$	0.2
$\Delta E_{(25'+48')}$	0.8
$\sum \Delta E_{pairs}$	−47.7
$\Delta E_{many\text{-}body}$ [a]	−2.5(5.0%)

[a] $\Delta E_{many\text{-}body} = \Delta E_{(SQV+25+25'+48+48')} - \sum \Delta E_{pairs}$.

atoms of the catalytic site residues leading to the conformational change of the D25 catalytic side chain. This is different from what observed for the D25′, in which its interactions with SQV in the WT of −16.1 kcal/mol and the G48V/L90M mutant of −16.3 kcal/mol are almost the same.

To examine the reliability of the calculated model where the many-body effects are almost neglected, the total and pairwise interactions for the (SQV + 25 + 25′ + 48 + 48′) complex of the WT were calculated separately and summarized in Table 4. The summation of the pairwise interaction energies of −47.7 kcal/mol is slightly higher than the complexation energy ($\Delta E_{(SQV+D25+25'+48+48')}$) of −50.2 kcal/mol. The discrepancy of about 5% is almost the same as that found for solvent–solvent interactions, which are normally neglected in classical simulations.

3.2. Stability of the WT, G48V and G48V/L90M complexes: ONIOM3 calculations

In this section, the interaction energies contributed from the residues in contact with the saquinavir and part of its binding pocket, as well as the entire protein, are included and treated by the ONIOM approach. Besides the highly accurate QM results applied for the *inner* region ($\Delta E_{[B3LPY,A]}$), the $\Delta\Delta E_{[PM3,AB\text{-}A]}$ and $\Delta\Delta E_{[UFF,ABC\text{-}AB]}$ shown in Table 5 represent the interactions contributed from the protein environment within the radius of 5 Å and the rest of the entire protein, respectively. Similar to the results for the QM calculations, substantial change was observed for the interaction energies yielded from the WT and G48V complexes, while a dramatic destabilization by 25.9 kcal/mol was observed for the double mutation, G48V/L90M (Table 5). Interestingly, the contribution of the interaction energies from the three ONIOM3 layers to the total enzyme–SQV interactions for WT and G48V are almost the same. The trend is $\Delta E_{[B3LPY,A]} > \Delta\Delta E_{[PM3,AB\text{-}A]} > \Delta\Delta E_{[UFF,ABC\text{-}AB]}$. This is not the case for G48V/L90M, where the largest contribution of 38% is from the *outer* layer which is the entire protein excluding the residues lying within the radius of 5 Å from all atoms of SQV (see also Fig. 3b).

3.3. Hydrogen bonding determination

The observation of the percent occupation of hydrogen bonding is based on the following criteria: (i) a distance between donor and acceptor heavy atoms $\leq$3.5 Å, (ii) an angle of donor-H-acceptor $\geq$120°. The simulation results are demonstrated in Fig. 5b. Distributions of the corresponding hydrogen bond distances, labeled as *d1–d6* in Fig. 4, are plotted in Fig. 5a. It can be seen that hydrogen bonds between SQV and the enzyme were observed in both the flap and catalytic regions. The comparison of the number, distance and percentage occupation between three systems (see Figs. 4 and 5) clearly indicate that the strength of hydrogen bonding is decreased by the mutation, especially the G48V/L90M double mutation.

In the catalytic region, three hydrogen bonds were formed for WT and G48V with 100% occupation (Fig. 5b). The corresponding O–H distances are 1.60 Å for *d1* and *d2* and 2.80 Å for *d3* (Fig. 5a). Two preferential conformations were observed for G48V/L90M indicated by the two peaks of the *d1–d3* distribution plots. This leads to the decrease of the occupation percentage because the hydrogen bond cannot be formed in the conformation represented by the second peak.

Table 5
The interaction energies representing the total (ΔE_{total}) and the three ONIOM3 layers according to Eq. (6) for the WT, G48V and G48V/L90M systems where percentage contributions from each layers to the total ΔE_{total} were also given

Systems	Interaction energy (kcal/mol)				
	WT	G48V	$\Delta\Delta E$ [a]	G48V/L90M	$\Delta\Delta E$ [b]
ΔE_{total}	−84.5	−87.0	−2.5	−58.6	25.9
$\Delta E_{[B3LYP,A]}$ [c]	−41.1 (49%)	−38.5 (44%)	2.6	−16.0 (27%)	25.1
$\Delta\Delta E_{[PM3,AB\text{-}A]}$ [d]	−27.0 (32%)	−30.8 (35%)	−3.8	−20.0 (34%)	7.0
$\Delta\Delta E_{[UFF,ABC\text{-}AB]}$ [e]	−16.4 (19%)	−17.7 (20%)	−1.3	−22.6 (38%)	−6.2

[a] $\Delta\Delta E = \Delta E_{G48V\ mutant} - \Delta E_{wild\text{-}type}$.
[b] $\Delta\Delta E = \Delta E_{G48V/L90M\ mutant} - \Delta E_{wild\text{-}type}$.
[c] $\Delta E_{[B3LYP,A]}$ accounts for interaction of SQV and D25/25′, G48/48′ and L90/90′.
[d] $\Delta\Delta E_{[PM3,AB\text{-}A]}$ represents interactions of SQV and the 5 Å surrounding residues, excluding D25/25′, G48/48′ and L90/90′.
[e] $\Delta E_{[UFF,ABC\text{-}AB]}$ represents interactions of SQV and the remaining residues.

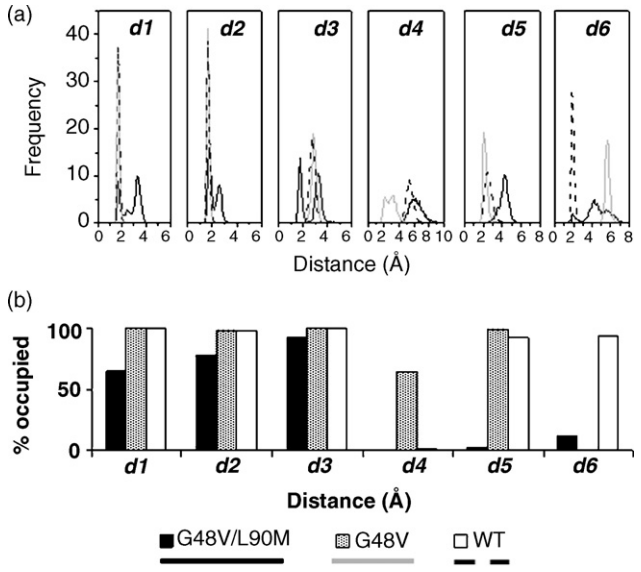

Fig. 5. (a) Distributions of the hydrogen bond distances (*d1–d6* in Fig. 4) and (b) the corresponding percentage occupation for the three simulated systems, the wild-type and G48V and G48V/L90M mutants.

For the flap region, the WT complex displays two hydrogen bonds with G48 indicated by *d5* and *d6* in Fig. 4, with almost 100% occupation plots (white for *d5* and *d6*) in Fig. 5b and sharp first peaks (dashed lines for *d5* and *d6*) in Fig. 5a. With the average O···H distance of *d4* = 5.36 Å (Fig. 5a, dashed line in *d4* plot), hydrogen bonding between the WT enzyme and the O atom at the P_2 subsite of SQV cannot be formed. Considering the single mutation at G48V, which is located at the flap region, the rotation of the P_2 subsite of saquinavir (see Fig. 4) has a strong influence comparison with the WT. One is the disappearance of hydrogen bonding formed between the NH-group of the P_2 subsite and the C=O peptide bond of the G48 backbone as indicated by the distance *d6* in Fig. 4 (see also the occupation and distribution plots in Fig. 5). In addition, rotation of the P_2 subsite also leads to the formation of the hydrogen bond between G48 and the O atom at the P_2 subsite of SQV.

The plot clearly shows that the G48V/L90M double mutation causes the much weaker hydrogen bonding formed between the SQV and the flap domain as indicated by broad distribution plots of *d4–d6* located at long distances (Fig. 5a). Only very low percentage occupations for *d5* and *d6* were observed throughout the simulations.

4. Conclusions

HIV-1 protease (PR) is an attractive target for antiviral therapy. Many substrate analog inhibitors have been designed, synthesized, and characterized. Among these, saquinavir (SQV) was the first HIV-1 PR inhibitor licensed for clinical use and is widely used for AIDS therapy. Its effectiveness, however, has been hindered by the emergence of resistant mutation, a common problem for inhibitors that target HIV-1 viral enzymes. Two important HIV-1 PR mutant species are the G48V single and G48V/L90M double mutants, associated *in vivo* with saquinavir resistance by the enzyme. Kinetic studies on these mutants demonstrate 13.5- and 419-folds increases in K_i values, respectively, compared with that of the wild-type. The analysis of energetic binding affinity between saquinavir and HIV-1 PR has been extensively performed based on DFT and QM/MM (ONIOM method) calculations. We have found that the interaction of SQV with the flap residue 48 significantly reduces the stability of binding between SQV and residue 48 for G48V and G48V/L90M compared with WT. This change is due to the loss of hydrogen bonding between the P_2 subsite of SQV and the backbone of residue 48. Moreover, the G48V/L90M mutation causes the repositioning of the residues close to residues 48 and 90 which are located in and play important roles as a part of the flap and catalytic regions, respectively. The implications of those results for the stabilization energy contributed by the catalytic site and protein effects, in comparison between WT and mutant systems are that (i) the disruption of the direct interaction between the drug and pocket, e.g., SQV–G48 and SQV–D25, by the mutated residue in direct contact (G48 → V) has the major effect to cause the significant change of the drug binding affinity, and (ii) a mutated residue such as L90 → M that is indirect contact with the drug can cause the repositioning of the protein structure, not only of the position in close contact but also throughout the entire protein. In addition to the loss of inhibitor/enzyme binding, it is interesting to observe that the mutation leads to a substantial increase of the stability of the enzyme.

Acknowledgment

We are very grateful to the Computational Chemistry Unit Cell and the Austrian–Thai Center for Computer Assisted Chemical Education and Research (ATC), Department of Chemistry, Faculty of Science, Chulalongkorn University, Thailand for computer resources. This work was supported by the Thailand Research Fund's Senior Scholar Grant no. RTA468008.

References

[1] B. Mahalingam, J.M. Louis, J. Hung, R.W. Harrison, I.T. Weber, Structural implications of drug-resistant mutants of HIV-1 protease: high-resolution crystal structures of the mutant protease/substrate analogue complexes, Proteins 43 (2001) 455–464.
[2] L. Hong, X.C. Zhang, J.A. Hartsuck, J. Tang, Crystal structure of an *in vivo* HIV-1 protease mutant in complex with saquinavir: insights into the mechanisms of drug resistance, Protein Sci. 9 (2000) 1898–1904.
[3] R.W. Shafer, P. Hsu, A.K. Patick, C. Craig, V. Brendel, Identification of biased amino acid substitution patterns in human immunodeficiency virus type 1 isolates from patients treated with protease inhibitors, J. Virol. 73 (1999) 6197–6202.
[4] C.F. Shuman, P.O. Markgren, M. Hamalainen, U.H. Danielson, Elucidation of HIV-1 protease resistance by characterization of interaction kinetics between inhibitors and enzyme variants, Antiviral Res. 58 (2003) 235–242.
[5] R. Kantor, W.J. Fessel, A.R. Zolopa, D. Israelski, N. Shulman, J.G. Montoya, M. Harbour, J.M. Schapiro, R.W. Shafer, Evolution of primary protease inhibitor resistance mutations during protease inhibitor salvage therapy, Antimicrob. Agents Chemother. 46 (2002) 1086–1092.

[6] A. Wlodawer, J.W. Erickson, Structure-based inhibitors of HIV-1 protease, Annu. Rev. Biochem. 62 (1993) 543–585.
[7] K. Wittayanarakul, O. Aruksakunwong, S. Saen-oon, W. Chantratita, V. Parasuk, P. Sompornpisut, S. Hannongbua, Insights into saquinavir resistance in the G48V HIV-1 protease: quantum calculations and molecular dynamic simulations, Biophys. J. 88 (2005) 867–879.
[8] J. Ermolieff, X. Lin, J. Tang, kinetic properties of saquinavir-resistant mutants of human immunodeficiency virus type 1 protease and their implications in drug resistance *in vivo*, Biochemistry 36 (1997) 12364–12370.
[9] W.L. Jorgensen, J. Chandrasekhar, J.D. Madura, R.W. Impey, M.L. Klein, Comparison of simple potential functions for simulating liquid water, J. Chem. Phys. 79 (1983) 926–935.
[10] J.M. Wang, W. Wang, P.A. Kollman, Antechamber: an accessory software package for molecular mechanical calculations, J. Am. Chem. Soc. 222 (2001) U403–U1403.
[11] C.I. Barly, P. Cieplak, W.D. Cornell, P.A. Kollman, A well-behaved electrostatic potential based method using charge restraints for determining atom-centered charges: the RESP model, J. Phys. Chem. 97 (1993) 10269–10280.
[12] W.D. Cornell, P. Cieplak, C.I. Bayly, P.A. Kollman, Application of RESP charges to calculate conformational energies, hydrogen-bond energies, and free-energies of solvation, J. Am. Chem. Soc. 115 (1993) 9620–9631.
[13] M.J. Frisch, G.W. Trucks, H.B. Schlegel, G.E. Scuseria, M.A. Robb, J.R. Cheeseman, V.G. Zakrzewski, J.A. Montgomery, J. Stratmann, J.C. Burant, S. Dapprich, J.M. Millam, A.D. Daniels, K.N. Kudin, M.C. Strain, O. Farkas, J. Tomasi, V. Barone, M. Cossi, R. Cammi, B. Mennucci, C. Pomelli, C. Adamo, S. Clifford, J. Ochterski, G.A. Petersson, P.Y. Ayala, Q. Cui, K. Morokuma, D.K. Malick, A.D. Rabuck, K. Raghavachari, J.B. Foresman, J. Cioslowski, J.V. Ortiz, A.G. Baboul, B.B. Stefanov, G. Liu, A. Liashenko, P. Piskorz, I. Komaromi, R. Gomperts, R.L. Martin, D.J. Fox, T. Keith, M.A. Al-Laham, C.Y. Peng, A. Nanayakkara, C. Gonzalez, M. Challacombe, P.M.W. Gill, B. Johnson, W. Chen, M.W. Wong, J.L. Andres, C. Gonzalez, M. Head-Gordon, E.S. Replogle, J.A. Pople, Gaussian 98, Gaussian, Inc., Pittsburgh, PA, 2002 .
[14] D.A. Case, J.W. Pearlman, T.E. Caldwell, J. Cheatham, W.S. Wang, C.L. Ross, T.A. Simmerling, K.M. Darden, R.V. Merz, A.L. Stanton, J.J. Cheng, M. Vincent, V. Crowley, H. Tsui, R.J. Gohlke, Y. Radmer, J. Duan, I. Pitera, G.L. Massova, U.C. Seibel, P.K. Singh, P.A. Kollman, AMBER 7.0, 2002.
[15] H.J.C. Berendsen, J.P.M. Postma, W.F.V. Gunsteren, A. DiNola, J.R. Haak, Molecular dynamics with coupling to an external bath, J. Chem. Phys. 81 (1984) 3684–3690.
[16] K. Morokuma, New challenges in quanum chemistry: quests for accurate calculations for large molecular systems, Philos. Trans. A Math. Phys. Eng. Sci. 360 (2002) 1149–1164.
[17] M. Torrent, T. Vreven, D.G. Musaev, K. Morokuma, O. Farkas, H.B. Schlegel, Effects of the protein environment on the structure and energetics of active sites of metalloenzymes. ONIOM study of methane monooxygenase and ribonucleotide reductase, J. Am. Chem. Soc. 124 (2002) 192–193.
[18] S. Saen-oon, M. Kuno, S. Hannongbua, Binding energy analysis for wild-type and Y181C mutant HIV-1 RT/8-C1 TIBO complex structures: quantum chemical calculations based on the ONIOM method, Proteins 61 (2005) 859–869.